

# RSC Advances



This is an *Accepted Manuscript*, which has been through the Royal Society of Chemistry peer review process and has been accepted for publication.

*Accepted Manuscripts* are published online shortly after acceptance, before technical editing, formatting and proof reading. Using this free service, authors can make their results available to the community, in citable form, before we publish the edited article. This *Accepted Manuscript* will be replaced by the edited, formatted and paginated article as soon as this is available.

You can find more information about *Accepted Manuscripts* in the [Information for Authors](#).

Please note that technical editing may introduce minor changes to the text and/or graphics, which may alter content. The journal's standard [Terms & Conditions](#) and the [Ethical guidelines](#) still apply. In no event shall the Royal Society of Chemistry be held responsible for any errors or omissions in this *Accepted Manuscript* or any consequences arising from the use of any information it contains.

**Random forest model for the ultrasonic-assisted removal of chrysoidine G by copper sulfide nanoparticles loaded on activated carbon; response surface methodology approach**

A. R. Bagheri<sup>a</sup>, M. Ghaedi<sup>a\*</sup>, S. Hajati<sup>b</sup>, A. M. Ghaedi<sup>c</sup>, A. Goudarzi<sup>d</sup>, A. Asfaram<sup>a</sup>

<sup>a</sup>Department of Chemistry, Yasouj University, Yasouj 75918-74831, Iran

<sup>b</sup>Department of Physics, Yasouj University, Yasouj 75918-74831, Iran

<sup>c</sup>Department of Chemistry, Gachsaran Branch, Islamic Azad University, Gachsaran 75818-63876, Iran

<sup>d</sup>Department of Polymer Engineering, Golestan University, Gorgan 49188-88369, Iran

\*Corresponding authors: Mehrorang Ghaedi

Tel/fax: Fax: +98-741-2223048

E-mail: m\_ghaedi@mail.yu.ac.ir; m\_ghaedi@yahoo.com

**Abstract:**

The copper sulfide nanoparticle-loaded activated carbon (CuS-NP-AC) was prepared and used as adsorbent for the accelerated removal of chrysoidine G (CG) assisted by ultrasound. This nanomaterial was characterized by FE-SEM, BET and XRD. The effects of variables such as initial CG concentration ( $\text{mg L}^{-1}$ ), adsorbent amount (g) and sonication time (s) on the CG removal were investigated and optimized by using central composite design (CCD) under response surface methodology (RSM). The Langmuir isotherm was applied to well describe the experimental equilibrium data with high figures of merit. The mass transfer mechanism of time varying adsorption was shown to be described by the second-order equation model. The random forest (RF) model applied to the experimental data was shown to be highly applicable to predict the CG adsorption onto CuS-NP-AC. The optimal tuning parameters for RF model were obtained based on 100 and 2 for  $n_{\text{tree}}$  and  $m_{\text{try}}$ , respectively. For the training data set, the values of MSE and the coefficient of determination ( $R^2$ ) were found to be 0.0021 and 0.9657, respectively, while they were obtained to be 0.0069 and 0.8976 for testing data set. It was found that a small adsorbent amount (0.03 g) is applicable for efficient removal of CG (RE > 94%) in short time (360 s) with reasonably high adsorption capacity ( $89.3 \text{ mg g}^{-1}$ ).

**Keywords:** Random forest model, Chrysoidine G, CuS Nanoparticles, Experimental design, Response surface methodology

## 1. Introduction

Chrysoidine G (CG) as industrial azoic dye (cationic dye)<sup>1</sup> is used for the construction of most textile dye stuffs and also synthetic industrial compounds.<sup>2,3</sup> The presence of azo dyes in most wastewater and aquatic media causes the generation of hazard to the aquatic life. CG as a synthetic azo dye (4-Phenylazo-m-phenylenediamine monohydrochloride) (See Table 1) known as a carcinogenic agent causes acute and chronic toxicity to mammals following consumption by oral or skin route.<sup>4</sup> Therefore, the CG removal through economical way is of high importance for the achievement of safe and clean media and ecosystem. Flocculation, coagulation, precipitation, adsorption, membrane filtration, electrochemical techniques, ozonation and biosorption have been extensively used for wastewater treatment.<sup>5</sup> The adsorption benefits from distinguished advantages such as high efficiency and capacity that candidate it for large-scale applicability, especially based on regenerable adsorbents.<sup>6-8</sup> Activated carbon (AC) with porous structure and various reactive sites is good candidate for dyes removal. It is most popular and low cost material for loading nanomaterial.<sup>9-12</sup> The presence of versatile functional groups including OH, -COOH, -C=O and amide groups permits simple and efficient loading of nanoparticles on its surface. This combination synergically improves their adsorption capacity and applicability for the rapid removal of dyes. Nanoparticles with high reactive atoms and large number of vacant metallic, semi-metallic or non-metallic reactive sites can be successfully applied for the removal of various toxic materials.<sup>13</sup> Composite nanoparticles such as copper sulfide nanoparticles loaded on activated carbon (CuS-NP-AC) improve the removal of organic and inorganic pollutants due to the presence of soft reactive atoms (copper and sulfide) and reactive centers. Ultrasound irradiations lead to increase in mass transfer through a liquid via different mechanisms such as convection pathway and generation of acoustic cavitations.<sup>14,15</sup> Shock waves may create microscopic turbulence within interfacial films surrounding neighbor solid particles.

Central composite design under response surface methodology as powerful optimization tool makes it possible to evaluate the effects of individual parameters and their possible interactions by running the least number of experiments.<sup>16-19</sup> Sonication time, amount of adsorbent and initial CG concentration were defined as independent variables which may affect the dye removal percentage as response.

Modeling used to solve complex engineering problems helps to analyze and understand real behavior of process and to confirm results obtained from the experiments. The selection of appropriate model is a key factor to accurately simulate the process. Interpretable multiple linear regressions (MLR)<sup>20</sup> and nonlinear protocol such as artificial neural networks (ANN)<sup>21</sup>,

fuzzy inference system (FIS),<sup>22</sup> adaptive neuro-fuzzy inference system (ANFIS) support vector machine (SVM), Gaussian process (GP)<sup>23</sup> and random forest (RF) are suitable pathways for modeling the adsorption and process. RF which is a relatively new nonlinear method, is used in classification and regression problems. The application of random forest (ensemble machine learning) improves the classification and regression trees (CART) method by the combination of hundreds of decision trees. The goal of the RF is to decrease the correlation between the individual trees by bootstrapping and randomized variable selection method, which results in diminished variance when the trees are aggregated. The random forest algorithm requires the tuning parameters;  $n_{\text{tree}}$  is the number of regression trees grown based on a bootstrap sample of the original data set (the default value is 500 trees);  $m_{\text{tree}}$  is the number of various predictors to try at each node (the default value is one third of the total number of the variables) and node size is the minimum size of terminal nodes.<sup>24</sup> The tree partitioning algorithm is constructed by recursively partitioning the larger space into two smaller spaces. The selection of split point is an optimization problem based on the squared error loss. An alternative way to think about the splitting process is that the algorithm begins with the root node. The algorithm splits is stopped when some stopping criteria is obtained. The most common stopping criterion is to keep the number of samples that fall in each region (Random forest-Matlab). The experimental data set is randomly divided into training and testing set. The inputs consist of initial CG concentration ( $\text{mg L}^{-1}$ ), amount of adsorbent (g) and sonication time (s). The output is the CG removal percentage (%). Inputs and outputs are normalized between 0 and 1 to avoid numerical overflows due to very large or small weights. This model can be successfully employed for the prediction of real behavior of many systems<sup>25-27</sup> by comparing the performance of random forest regression against the stepwise multiple linear regression.<sup>28,29</sup>

## 2. Experimental

### 2.1. Materials and methods

All chemicals including CG, NaOH and HCl with the highest purity available were purchased from Merck company (Darmstadt, Germany). All laboratory equipments and instruments including an ultrasonic bath with heating system, pH measurements, UV-Vis spectrophotometer as well as equations and concepts used for the calculation of removal percentage and adsorption capacity were fully presented in previous reports.<sup>30,31</sup>

X-ray diffraction (XRD, Philips PW 1800) was performed to characterize the phase and structure of the prepared nanoparticles using  $\text{Cu}_{\text{K}\alpha}$  radiation (40 KV and 40 mA) over  $2\theta$  range

of 15-70°. The morphology of the nanoparticles was observed by field emission scanning electron microscopy (FE-SEM: Hitachi S- 4160) under an acceleration voltage of 20 and 30 KV. The stock solution (200 mg L<sup>-1</sup>) of CG was prepared by dissolving 20 mg of solid dye in 100 mL double distilled water and the working concentrations were daily prepared by their suitable dilution.

### 2.2. Preparation of copper sulfide nanoparticles

Copper (II) acetate (Cu (CH<sub>3</sub>COO)<sub>2</sub> · 2H<sub>2</sub>O) and thioacetamide (CH<sub>3</sub>CSNH<sub>2</sub>) were used for supplying Cu<sup>2+</sup> and S<sup>2-</sup> ions. The CuS nanoparticle-loaded activated carbon (CuS-NP-AC) was prepared as follows: 10 mL of 0.02 mol L<sup>-1</sup> copper (II) acetate solution was diluted using 190 mL distilled water. Then, 2.5 g activated carbon (AC) was added to the mixture and stirred thoroughly. The dropwise addition of 60 mL of 0.0067 mol L<sup>-1</sup> thioacetamide while stirring during 30 minutes at 30 °C and subsequently keeping at room temperature for 1 h led to the formation of CuS-NP-AC. The solid material was filtered and washed for several times by distilled water to produce pure CuS-NP-AC. It was dried at 60 °C for 3 h and applied as adsorbent for adsorption experiments.

### 2.3. Central composite design (CCD)

Generally, experimental design is applicable for the simultaneous optimization of variables to improve the performance of adsorption process and to minimize error<sup>32,33</sup> with least number of runs. The 20 CCD runs and their corresponding responses are presented in Table 2. The amount of adsorbent (X<sub>1</sub>), initial CG concentration (X<sub>2</sub>) and sonication time (X<sub>3</sub>) are given for each experimental run. The details on desirability function (DF) and RSM were presented in previous reports.<sup>34</sup>

## 3. Results and discussion

### 3.1. $pH_{zpc}$

Distribution of AC charge plays a key role in the removal of dyes and their interaction to adsorbent. The intersection of surface with solute ions or molecules is dependent on the adsorbent charge (positive and negative) which alters the mechanism and corresponding forces. Adsorbent surface is neutral at pH identified as zero point of charge ( $pH_{zpc}$ ). In addition, the remarkable mechanism for solute transfer is considered to be the diffusion into the adsorbent. At pH above  $pH_{zpc}$ , the adsorbent surface charge changes into negative and thus the positive ions are absorbed on the surface based on electrostatic attraction while the reverse

occurs at the pH below this value.<sup>35</sup> The calculated value of  $pH_{zpc}$  (1.7) shows high tendency of the CG dye for strong adsorption on the surface of CuS-NP-AC.

### 3.2. Effect of pH on the removal efficiency

The initial pH has distinguished effect on the dye adsorption and the surface binding sites of the adsorbent. CuS-NP-AC showed maximum percentage of the removal of CG at pH 6.0. At lower pH, the various functional groups and reactive atom of CG as well as adsorbent is protonated and both get positive charge. Therefore, due to the strong repulsive force between dye and adsorbent surface the dye removal percentage decreases. Increasing pH from 2.0 to 6.0 improves the removal percentage from 84 to 90 % (Fig. 1 ).

### 3.3. Characterization of adsorbent

Field emission scanning electron microscopy (FE-SEM) under an acceleration voltages of 20 and 30 KV gives FE-SEM images of CuS-NP-AC with different magnifications (Figs. 2A and 2B) confirming the homogeneous distribution of spherical like nanoparticles with diameters in the range 50-100 nm.

The XRD pattern of CuS-NP-AC (Fig. 2C) shows a broad hump at  $2\theta=20-25^\circ$  and a broad peak at  $2\theta=43^\circ$  corresponding to the amorphous nature of activated carbon modified with CuS nanoparticles. The BET surface area of the adsorbent was obtained to be  $788.5 \text{ m}^2 \text{ g}^{-1}$ . The adsorption-desorption isotherm was studied using nitrogen gas which showed no porosity (Fig.3)<sup>36</sup>.

### 3.4. Central composite design (CCD)

The three independent variables of adsorbent dosage ( $X_1$ ), CG concentration ( $X_2$ ) and sonication time ( $X_3$ ) involved in CCD were considered in five levels (Table 2). The experimental response corresponding to each run was estimated and the analysis of variance (ANOVA) was performed using Design Expert 7.0 software to give useful information on the level of significance of each variable in addition to their interaction (Table 3). The judgment on the significance of each term is based on *p-value* less than 0.05 at 95 % confidence level. Data analysis gave the following semi-empirical expression to model the CG removal percentage ( $R\%_{CG}$ ):

$$R\%_{CG} = 87.99 + 8.20X_1 - 6.90X_2 + 7.85X_3 + 2.31X_1X_2 + 2.74X_1X_3 + 3.76X_2X_3 - 7.98X_1^2 - 1.69X_2^2 - 317X_3^2 \quad (1)$$

The model p-value was found to be less than 0.05 which implies its significance. Furthermore, the "Lack of Fit p-value" was obtained to be 0.1129 which implies that the "Lack of Fit" is not significant. Thus the model is well applicable for the prediction of experimental data. "Adeq Precision" measures the signal to noise ratio while the ratio greater than 4 is desirable. It was obtained to be 50.029 that confirms its adequacy for the explanation of signal. The plot of experimental removal percentage (%) versus the predicted values showed good agreement Fig. (4).

### 3.5. Response surface methodology

Fig.5 (a–c) represents the most relevant fitted response surfaces for the design depicting the response surface plots of R%<sub>CG</sub> versus significant variables. These plots were obtained for a given pair of factors at fixed optimal values of other variables. Figs. 5a and 5b present the interaction of CG concentration with sonication time and adsorbent dosage, respectively. As it was expected, the dye removal percentage was positively correlated to the sonication time and adsorbent mass. High contribution of ultrasound in the enhancement of mass transfer made it possible to achieve a rapid adsorption process which is an advantage of this research. In addition, the ultrasound application leads to more efficient dispersion of adsorbent in liquid phase (aqueous media) and supplies more reactive centers on the adsorbent surface for the dye adsorption (Fig. 5b). At higher dye concentrations, adsorption yield decreases due to the saturation of adsorption sites.

### 3.6. Optimization of CCD by DF

The profile for predicted values and desirability option in the Design Expert software were used to optimize the adsorption process. The scale in the range of 0.0 (undesirable) to 1.0 (very desirable) is used for the judgment on global function (DF) as best criterion for the optimization of designed variables. The minimum and maximum of R%<sub>CG</sub> in CCD (Table 2) were found to be 50.10 and 94.00 %, respectively. The maximum dye removal percentage was found to be achieved at the following condition: 0.03 g of CuS-NP-AC, 19.45 mg L<sup>-1</sup> of CG, pH=6 and 360 s sonication time with desirability 1.0.



### 3.7. Adsorption equilibrium study

Various models such as Langmuir, Freundlich, Temkin and Dubinin– Radushkevich (D–R) isotherms were applied to describe the experimental equilibrium data. The constant parameters corresponding to each model were obtained (Table 4) and the efficiency of each model was judged according to their value and the correlation coefficient ( $R^2$ ). Based on the linear form of Langmuir isotherm model (Table 4), the values of  $K_a$  (the Langmuir adsorption constant ( $L\ mg^{-1}$ )) and  $Q_m$  (the maximum monolayer adsorption capacity ( $mg\ g^{-1}$ )) are proportional to the intercept and slope of linear plot of  $q_e$  versus  $C_e$ , respectively (Table 4). The fitness of experimental data was evaluated at different levels of adsorbent dosage. The high correlation coefficients at all adsorbent dosages suggest the well applicability of Langmuir model for the interpretation of the experimental data over the whole concentration range. The essential characteristics of the Langmuir isotherm can be expressed in terms of a dimensionless constant known as separation factor ( $R_L$ ) that is given by the following equation.<sup>37</sup>

$$R_L = \frac{1}{1 + K_a C_0} \quad (2)$$

There are four possible cases for the  $R_L$  value: for favorable sorption,  $0 < R_L < 1$ ; for unfavorable sorption,  $R_L > 1$ ; for linear sorption,  $R_L = 1$ ; for irreversible sorption,  $R_L = 0$ .<sup>38,39</sup> As shown in Table 4, the Freundlich parameters including the adsorption capacity ( $K_f$  ( $L\ mg^{-1}$ )) and intensity ( $1/n$ ) were calculated from the intercept and slope of the linear plot of  $\ln q_e$  versus  $\ln C_e$ , respectively. The values of  $1/n$  (0.456, 0.410 and 0.360) obtained from Freundlich isotherm show the high tendency of CG for the adsorption onto CuS-NP-AC, while lower  $R^2$  values (0.931, 0.958 and 0.938) corresponding to the adsorbent dosage of 0.01, 0.015 and 0.02 g show its unsuitability for fitting the experimental data over the whole concentration range. The heat of adsorption and the adsorbent–adsorbate interaction were evaluated by applying Temkin isotherm model.<sup>40,41</sup> The correlation coefficient corresponding to Temkin was found to be lower than that of the Langmuir. Therefore, it was shown that the Temkin isotherm represents a worse fit to the experimental data while the Langmuir isotherm applies well. D–R model was applied to estimate the porosity apparent free energy and the characteristics of adsorption. In the D–R isotherm  $K$  ( $mol^2\ (K\ J^2)^{-1}$ ) is a constant related to the adsorption energy,  $Q_s$  ( $mg\ g^{-1}$ ) is the theoretical saturation capacity and  $\epsilon$  is the Polanyi potential. The slope of the plot of  $\ln q_e$  versus  $\epsilon^2$  gives  $K$  and the intercept yields the  $Q_s$  value

(Table 4). The values of correlation coefficient obtained from D–R model (0.951, 0.929 and 0.963) are lower than that of Langmuir isotherm (Table 4). This means that the D–R equation represents not better fit to the experimental data than the Langmuir isotherm. Thus, the best applicable model was Langmuir. This means that the adsorption of CG dye takes place as a mono-layer at specific homogeneous sites onto CuS-NP-AC surface.

### 3.8. Adsorption kinetics

In adsorption process, it is important to obtain useful knowledge about its rate and suitable equation which applies. The conventional models which may apply to describe the adsorption kinetics are summarized in Table 5. The pseudo-first-order model (Lagergren model) is based on the plot of  $\log(q_e - q_t)$  versus  $t$  from the slope and intercept of which  $K_1$  and  $q_e$  are calculated, respectively (Table 5).<sup>42,43</sup> As seen, the experimental  $q_e$  is not consistent with the calculated one which implies that the pseudo-first-order model is not applicable. The increase in the value of  $K_1$  and  $K_2$  is attributed to the increase in mass transfer.<sup>44</sup> The sorption kinetics may be described by a pseudo second-order model.<sup>45</sup> In spite of the first order model, the plot of  $t/q_t$  versus  $t$  for the pseudo-second-order kinetic model gives a straight line with high correlation coefficient. It shows that the theoretical and experimental  $q_e$  are in good agreement. In other words, the pseudo-second-order kinetic model describes the experimental data well. The Elovich equation is based on tracing  $q_t$  versus  $\ln(t)$  which gives a linear relationship with a slope of  $(1/\beta)$  and an intercept of  $(1/\beta) \ln(\alpha\beta)$ .<sup>46</sup> In most cases, in addition to the above-mentioned mechanism, the intraparticle diffusion model based on square root of time ( $t$ ) is used to predict real behavior of adsorption system.<sup>47,48</sup> The values of  $K_{diff}$  and  $C$  were calculated from the slope and intercept of the plot of  $q_t$  versus  $t^{1/2}$ , respectively.  $C$  value is related to the thickness of the boundary layer and  $K_{diff}$  is the intraparticle diffusion rate constant ( $\text{mg g}^{-1} \text{min}^{-1/2}$ ) (Table 5). The deviation of intercept value from zero confirms a cooperative mechanism for reaction that is composed of the pseudo-second order and intraparticle diffusion controlling the mass transfer from bulk to the external surface and lateral diffusion to the internal pores of adsorbent.

### 3.9. Random forest model

Random forest (RF) has three tuning parameters including  $n_{tree}$ ,  $m_{tree}$  and extra options. Table 6 shows the range tuning parameters and the coefficient of determination ( $R^2$ ) obtained as well as MSE for the training and testing sets. The results show that the optimal tuning parameters for RF model are achieved based on the  $n_{tree}=100$ ,  $m_{tree}=2$  and the default extra-

options (with replacement) in the forest. In optimal model, the training and testing sets which are here the MSE values of 0.0021 and 0.0069, with  $R^2$  values of 0.9657 and 0.8976, respectively. The Out of Bag (OOB) error rate versus number of trees (Fig. 6) shows that the out of bag error rate converges until 100 trees and remains constant at higher number. Table 6 shows the MSE and  $R^2$  of the RF model for training and testing sets.

### 3.10. Comparison with other methods

The operation of the proposed method is comparable to other methods<sup>49,50</sup> as well as to some adsorbents (Table 7). The findings show that our study is superior to the other studies in terms of the adsorption capacity for the removal of CG, thus preferred. Moreover, it has been suggested that the ultrasound-assisted method for the dye removal is considered as an efficient method because this method is linked to the high-pressure shock waves in addition to the high-speed microjets throughout the violent collapse of cavitation bubbles.

## 4. Conclusion

It was observed that the combination of ultrasonic waves with CuS-NP-AC is an efficient, fast and sensitive adsorption method for the removal of CG dye. The adsorption capacity of the applied adsorbent was found to be  $89.3 \text{ mg g}^{-1}$ . The influences of experimental parameters on the CG removal percentage were successfully investigated by experimental design methodology. The isotherm models such as Langmuir, Freundlich, and Temkin were evaluated and it was shown that the equilibrium data were best described by the Langmuir model. The process kinetics was successfully fitted to the pseudo-second-order kinetic model. In the present investigation, a RF model was developed as an efficient tool for the prediction of CG adsorption onto CuS-NP-AC. The results show that there is a good agreement between experimental data and the data predicted by presented RF model. More than 94 % of the CG was removed by using small amount of adsorbent (0.03 g) in very short time (360 s).

**References**

1. K. Doh-ura, K. Tamura, Y. Karube, M. Naito, T. Tsuruo, Y. Kataoka, *Cell. Mol. Neurobiol.*, 2007, **27**, 303-316.
2. G.B. Michaels, D.L. Lewis, *Environ. Toxicol. Chem.*, 1986, **5**, 161-166.
3. K.T. Chung, S.E. Stevens, *Environ. Toxicol. Chem.*, 1993, **12**, 2121-2132.
4. T. Reyns, S. Fraselle, D. Laza, J. Van Loco, *Biomed. Chromatogr.*, 2010, **24**, 982-989.
5. S. Khodadoust, M. Ghaedi, R. Sahraei, A. Daneshfar, *J. Ind. Eng. Chem.*, 2014, **20**, 2663-2670.
6. M. Ghaedi, B. Sadeghian, S.N. Kokhdan, A.A. Pebdani, R. Sahraei, A. Daneshfar, A. Mihandoost, *Materials Sci. Eng. C*, 2013, **33**, 2258-2265.
7. S. Hajati, M. Ghaedi, F. Karimi, B. Barazesh, R. Sahraei and A. Daneshfar, *J. Ind. Eng. Chem.*, 2014, **20**, 564-571.
8. S. Hajati, M. Ghaedi, B. Barazesh, F. Karimi, R. Sahraei, A. Daneshfar and A. Asghari, *J. Ind. Eng. Chem.*, 2014, **20**, 2421-2427.
9. G. Mezohegyi, F.P. van der Zee, J. Font, A. Fortuny, A. Fabregat, *J. environ. management*, 2012, **102**, 148-164.
10. R.S. Ribeiro, N.A. Fathy, A.A. Attia, A.M. Silva, J.L. Faria, H.T. Gomes, *Chem. Eng. J.*, 2012, **195**, 112-121.
11. M. Roosta, M. Ghaedi, A. Daneshfar, R. Sahraei, *Spectrochim. Acta Part A*, 2014, **122**, 223-231.
12. M. Ghaedi, K. Mortazavi, M. Jamshidi, M. Roosta, B. Karami, *Toxic. Environ. Chem.*, 2012, **94**, 846-859.
13. M. Ghaedi, M.D. Ghazanfarkhani, S. Khodadoust, N. Sohrabi, M. Oftade, *J. Ind. Eng. Chem.*, 2014, **20**, 2548-2560.
14. G.L. Maddikeri, A.B. Pandit, P.R. Gogate, *Ind. Eng. Chem. Res.*, 2012, **51**, 6869-6876.
15. B.R. Reddy, T. Sivasankar, M. Sivakumar, V.S. Moholkar, *Ultrasonics sonochem.*, 2010, **17**, 416-426.
16. A. Asfaram, M. Ghaedi, S. Agarwal, I. Tyagi, V. Kumar Gupta, *RSC Adv.*, 2015, **5**, 18438-18450.
17. M. Ghaedi, A. Shahamiri, B. Mirtamizdoust, S. Hajati and F. Taghizadeh, *Spectrochim. Acta, Part A*, 2015, **138**, 878-884.
18. M. Ghaedi, E. Alam Barakat, A. Asfaram, B. Mirtamizdoust, A.A. Bazrafshan and S. Hajati, *RSC Adv.*, 2015, **5**, 42376-42387.
19. M. Ghaedi, S. Hajati, M. Zare, M. Zare, S.Y. Shajaripour Jaber, *RSC Adv.*, 2015, **5**, 38939-38947.
20. U. Özdemir, B. Özbay, S. Veli, S. Zor, *Chem. Eng. J.*, 2011, **178**, 183-190.

21. S. Elemen, E.P.A. Kumbasar, S. Yapar, *Dye. Pigm.*, 2012, **95**, 102-111.
22. M. Razani, A. Yazdani-Chamzini, S.H. Yakhchali, *Safety Sci.*, 2013, **55**, 26-33.
23. Y. Liu, F. Sun, *Expert Syst Appl.*, 2013, **40**, 4496-4502.
24. M. Ghaedi, A.M. Ghaedi, E. Negintaji, A. Ansari, A. Vafaei, M. Rajabi, *J. Ind. Eng. Chem.*, 2014, **20**, 1793-1803.
25. Y. Heo, V.M. Zavala, *Energy and Buildings*, 2012, **53**, 7-18.
26. A. Hapfelmeier, K. Ulm, *Comput. Stat. Data Anal.*, 2013, **60**, 50-69.
27. M. Pardo, G. Sberveglieri, *Sens. Actuators B Chem.*, 2008, **131**, 93-99.
28. O. Mutanga, E. Adam, M.A. Cho, *Int. J. Appl. Earth Obs. Geoinf.*, 2012, **18**, 399-406.
29. M.H. Schwartz, A. Rozumalski, W. Truong, T.F. Novacheck, *Gait posture*, 2013, **37**, 473-479.
30. M. Ghaedi, M. Pakniat, Z. Mahmoudi, S. Hajati, R. Sahraei, A. Daneshfar, *Spectrochim. Acta Part A*, 2014, **123**, 402-409.
31. R. Hosseini Nia, M. Ghaedi, A.M. Ghaedi, *J. Mol. Liq.*, 2014, **195**, 219-229.
32. S. Hajati, M. Ghaedi and S. Yaghoubi, *J. Ind. Eng. Chem.*, 2015, **21**, 760-767.
33. M. Roosta, M. Ghaedi, M. Mohammadi, *Pow. Tech.*, 2014, **267**, 134-144.
34. A. Asfaram, M. Ghaedi, S. Hajati, A. Goudarzi, A.A. Bazrafshan, *Spectrochim. Acta Part A*, 2015, **145**, 203-212.
35. M. Ghaedi, H. Mazaheri, S. Khodadoust, S. Hajati, M.K. Purkait, *Spectrochim. Acta Part A*, 2015, **135**, 479-490.
36. X. Zhu and Y.-P. Zhao, *J. Phys. Chem. C*, 2014, **118**, 17737-17744.
37. S.Z. Mohammadi, M.A. Karimi, D. Afzali, F. Mansouri, *Desalination*, 2010, **262**, 86-93.
38. H. Zheng, D. Liu, Y. Zheng, S. Liang, Z. Liu, *J. Hazard. Mater.*, 2009, **167**, 141-147.
39. M. Mathivanan, E. Saranathan, *J. Chem. Pharmaceutical Res.*, 2015, **7**, 817-822.
40. O. Amuda, A. Giwa, I. Bello, *Biochem. Eng. J.*, 2007, **36**, 174-181.
41. J. Fu, Z. Chen, M. Wang, S. Liu, J. Zhang, J. Zhang, R. Han, Q. Xu, *Chem. Eng. J.*, 2015, **259**, 53-61.
42. I. Guerrero-Coronilla, L. Morales-Barrera, E. Cristiani-Urbina, *J. Environ. Management*, 2015, **152**, 99-108.
43. M. Ghaedi, H. Khajesharifi, A. Hemmati Yadkuri, M. Roosta, R. Sahraei, A. Daneshfar, *Spectrochim. Acta Part A*, 2012, 86 62-68.
44. Y.S. Ho, G. McKay, *Chem. Eng. J.*, 1998, **70**, 115-124.

45. Y.S. Ho, G. McKay, *Process Biochem.*, 1999, **34**, 451-465.
46. K. Ahmadi, M. Ghaedi, A. Ansari, *Spectrochim. Acta Part A*, 2015, **136**, 1441-1449.
47. S. Nethaji, A. Sivasamy, *Chemosphere*, 2011, **82**, 1367-1372.
48. D. Ozdes, C. Duran, H.B. Senturk, *J. environ. management*, 2011, **92**, 3082-3090.
49. A. Mittal, J. Mittal, A. Malviya, V. Gupta, *J. Col. Interface Sci.*, 2010, **344**, 497-507.
50. V.M. Nurchi, M. Crespo-Alonso, R. Biesuz, G. Alberti, M.I. Pilo, N. Spano, G. Sanna, *Arabian J. Chem.*, 2014, **7**, 133-138.

---

**Figure captions:**

---

**Fig. 1.** Effect of pH on the adsorption of CG onto CuS-NP-AC in the range of 2–8. (General condition: adsorbent dosage: 0.01 g, SS: 3000 rpm, T: 298.15 K, Ultrasonic time (min): 3 min, in 50 mL dye solution: CG concentration: 10 mg L<sup>-1</sup>).

**Fig. 2.** (a) and (b). FE-SEM images of the prepared CuS-NP-loaded AC at different magnifications. (c) XRD pattern of the prepared CuS-NP-AC.

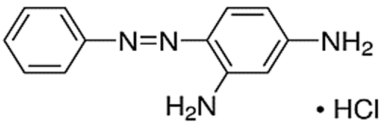
**Fig. 3.** Adsorption-desorption isotherm using nitrogen.

**Fig.4.** The experimental data versus the predicted data of normalized removal of CG.

**Fig.5.** Response surfaces for the Removal of CG (R%) by CuS-NP-AC: (a) initial CG concentration-Sonication time; (b) initial CG concentration- Adsorbent dosage; (c) Adsorbent dosage-Sonication time.

**Fig.6.** The OOB error rate versus number of trees.

**Table 1.** Physical properties and molecular structure of CG.

Name	Chrysoidine G (CG)
CAS Number	532-82-1
Molecular Structure	
Chemical Formula	$C_{12}H_{13}N_4Cl$
Molecular Weight	$248.71 \text{ g mol}^{-1}$
Maximum wavelength ( $\lambda_{\text{max}}$ ), nm	461
Use	Textile industry
Class	Azo
Color	Orange



**Table 2.** Experimental factors and levels in the central composite design

Factors	Levels			Star point $\alpha=1.68$	
	Low (-1)	Centra (0)	High (+1)	$-\alpha$	$+\alpha$
(X <sub>1</sub> ) Adsorbent dosage (g)	0.012	0.0225	0.033	0.005	0.05
(X <sub>2</sub> ) CG concentration (mg L <sup>-1</sup> )	9	15	21	5	25
(X <sub>3</sub> ) Sonication time (s)	120	240	360	38	442
Run	(X <sub>1</sub> )	(X <sub>2</sub> )	(X <sub>3</sub> )	R% CG	
1	0.0120	21	360	65.80	
2	0.0120	21	120	50.10	
3	0.0225	15	442	92.60	
4 (C)	0.0225	15	240	89.00	
5	0.0120	9	360	79.00	
6	0.0120	9	120	75.00	
7 (C)	0.0225	15	240	87.00	
8	0.0225	15	38	65.30	
9	0.0225	5	240	94.00	
10	0.0330	21	360	93.00	
11	0.0330	9	120	82.00	
12	0.0400	15	240	80.33	
13	0.0225	21	120	63.00	
14 (C)	0.0225	15	240	87.00	
15 (C)	0.0225	15	240	88.00	
16	0.0225	25	240	72.50	
17 (C)	0.0225	15	240	88.00	
18 (C)	0.0225	15	240	89.00	
19	0.0050	15	240	50.93	
20	0.0330	9	360	93.60	

(C): Center point

**Table 3.** Analysis of variance for removal of CG (R%) by CuS-NP-AC

Source of variation	Sum of square	Degree of freedom	Mean square	F-value	P-value
X <sub>1</sub>	915.28	1	915.28	542.82	< 0.0001
X <sub>2</sub>	905.05	1	905.05	536.76	< 0.0001
X <sub>3</sub>	645.38	1	645.38	382.76	< 0.0001
X <sub>1</sub> <sup>2</sup>	39.98	1	39.98	23.71	0.0007
X <sub>2</sub> <sup>2</sup>	841.70	1	841.70	499.18	< 0.0001
X <sub>3</sub> <sup>2</sup>	145.75	1	145.75	86.43	< 0.0001
X <sub>1</sub> X <sub>2</sub>	42.78	1	42.78	25.37	0.0005
X <sub>1</sub> X <sub>3</sub>	59.95	1	59.95	67.17	0.0001
X <sub>2</sub> X <sub>3</sub>	113.25	1	113.25	35.56	< 0.0001
Lack of fit	12.82	5	2.57	3.22	0.1129
Pure error	4.00	5	0.80		
Total SS	3617.87	19			

**Table 4.** Comparison of the isotherm parameters for CG adsorption onto CuS-NP-AC at optimum conditions

Isotherm	Equation	Parameters	Adsorbent (g)		
			0.01	0.015	0.02
Langmuir	$C_e/q_e = 1/(K_a Q_m) + C_e/Q_m$	$Q_m$ (mg g <sup>-1</sup> )	89.3	61.4	48.2
		$K_a$ (L mg <sup>-1</sup> )	0.419	0.552	1.12
		$R_L$	0.074-0.323	0.057-0.256	0.030-0.151
		$R^2$	0.993	0.998	0.999
Freundlich	$\ln q_e = \ln K_F + (1/n) \ln C_e$	$1/n$	0.456	0.410	0.360
		$K_F$ (L mg <sup>-1</sup> )	4.12	3.472	3.76
		$R^2$	0.931	0.958	0.938
		$B_1$	20.3	12.8	9.30
Temkin	$q_e = B_1 \ln K_T + B_1 \ln C_e$	$K_T$ (L mg <sup>-1</sup> )	3.63	5.70	13.5
		$R^2$	0.996	0.989	0.986
		$B_1$	20.3	12.8	9.30
Dubinin and Radushkevich	$\ln q_e = \ln Q_m - K\varepsilon^2$	$Q_m$ (mg g <sup>-1</sup> )	70.8	48.2	41.4
		$K \times 10^{-7}$	3.00	2.00	0.90
		$R^2$	0.951	0.929	0.963

**Table 5.** Kinetics parameters of CG adsorption onto CuS-NP-AC

Model	Concentration dye (mg L <sup>-1</sup> )	Parameter values of the CG adsorption					
		15	50	15	50	30	50
	Adsorbent (g)	0.02	0.02	0.01	0.01	0.03	0.05
First order kinetic model: $\log(q_e - q_t) = \log(q_e) - (K_1/2.303)t$	$K_1$ (min <sup>-1</sup> )	0.345	0.284	0.481	0.390	0.637	0.405
	$q_e$ (cal.) (mg g <sup>-1</sup> )	9.60	8.16	15	125	67.2	14.4
	$R^2$	0.939	0.995	0.435	0.971	0.941	0.940
Second order kinetic model: $(t/q_t) = 1/K_2q_e^2 + (1/q_e)t$	$K_2$ (min <sup>-1</sup> )	0.050	0.060	0.005	0.001	0.009	0.040
	$q_e$ (cal.) (mg g <sup>-1</sup> )	37.87	70.7	86.2	222	62.5	51.3
	$R^2$	0.998	0.999	0.990	0.980	0.999	0.997
Intraparticle diffusion $q_t = K_{diff}t^{1/2} + C$	$h$	71.70	372	37.2	34.56	35.15	105
	$K_{diff}$ (mg g <sup>-1</sup> min <sup>-1/2</sup> )	3.67	3.80	19.6	54.3	13.6	4.83
	$C$ (mg g <sup>-1</sup> )	25.8	66.8	13.2	18.3	14.6	35.5
	$R^2$	0.995	0.994	0.998	0.996	0.974	0.997
Elovich $q_t = 1/\beta \ln(\alpha\beta) + 1/\beta \ln(t)$	$\beta$	0.279	0.270	0.052	0.019	0.074	0.212
	(mg g <sup>-1</sup> min <sup>-1</sup> ) $\alpha$	9626	50868	76.4	79.5	78.4	17725
	$R^2$	0.975	0.979	0.984	0.982	0.997	0.981
Experimental data	$Q_e$ (exp) (mg g <sup>-1</sup> )	36.7	77.2	65.2	117	49.3	48.3

**Table 6.** The range of tuning parameters and obtained statistical data for training and testing data sets.

	n <sub>tree</sub>	m <sub>try</sub>	Extra options	Training Set		Testing Set	
				R <sup>2</sup>	MSE	R <sup>2</sup>	MSE
1	500	1	-	0.9329	0.0063	0.8030	0.0156
2	100	1	-	0.9231	0.0067	0.8235	0.0151
3	100	2	-	0.9624	0.0022	0.8836	0.0071
<sup>1</sup> 4	500	1	-	0.9334	0.0061	0.8339	0.0141
<sup>2</sup> 5	100	4	Without replacement	0.9151	0.0037	0.7802	0.0105
6	100	4	sampsiz = size(X <sub>trn</sub> ,1)*2/3	0.9087	0.0091	0.8330	0.0142
<sup>3</sup> 7	100	4	nodesize = 7	0.9244	0.0066	0.8305	0.0141
<sup>4</sup> 8	100	4	importance = 1	0.9521	0.0052	0.8656	0.0141
<sup>4</sup> 9	100	4	localImp=1	0.9146	0.0063	0.8197	0.0142
<sup>4</sup> 10	100	4	proximity = 1	0.9288	0.0062	0.8492	0.0150
<sup>5</sup> 11	100	4	proximity = 1, oob <sub>prox</sub> = 0	0.9538	0.0054	0.8725	0.0124
<sup>4</sup> 12	100	4	do <sub>trace</sub> = 1	0.9172	0.0065	0.8191	0.0136
<sup>4</sup> 13	100	4	In bag = 1	0.9457	0.0054	0.8778	0.0128
<sup>4</sup> 14	100	2	importance=1, nPerm = 1	0.9396	0.0059	0.8374	0.0140
15	100	2	importance=1, nPerm = 3	0.9657	0.0021	0.8976	0.0069

<sup>1</sup> Set to defaults trees and m<sub>try</sub> by specifying values as 0

<sup>2</sup> Set sampling without replacement (default is with replacement)

<sup>3</sup> Note that the default value is 5 for regression

<sup>4</sup> Default (Don't) = 0

<sup>5</sup> Default = 1 if proximity is enabled, Don't 0

**Table 7.** Comparison for the removal of CG by different methods and adsorbents.

Adsorbent	Adsorption capacity ( $\text{mg g}^{-1}$ )	References
Botton ash	18.08	49
De-oiled soya	8.33	49
Row cork	57.3	50
CuS-NPs-AC	89.3	This work

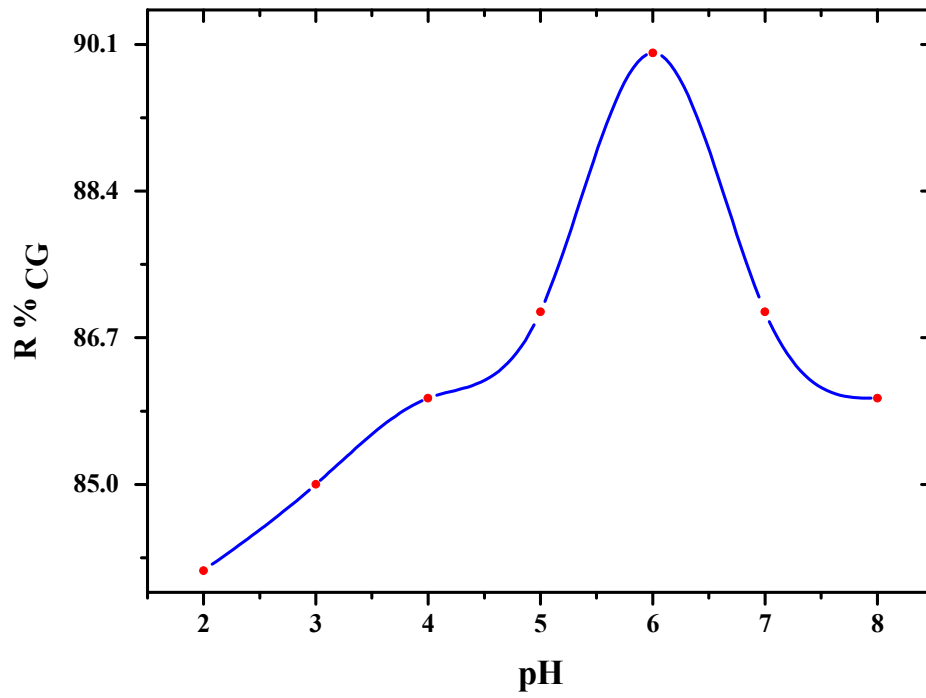


Fig. 1.

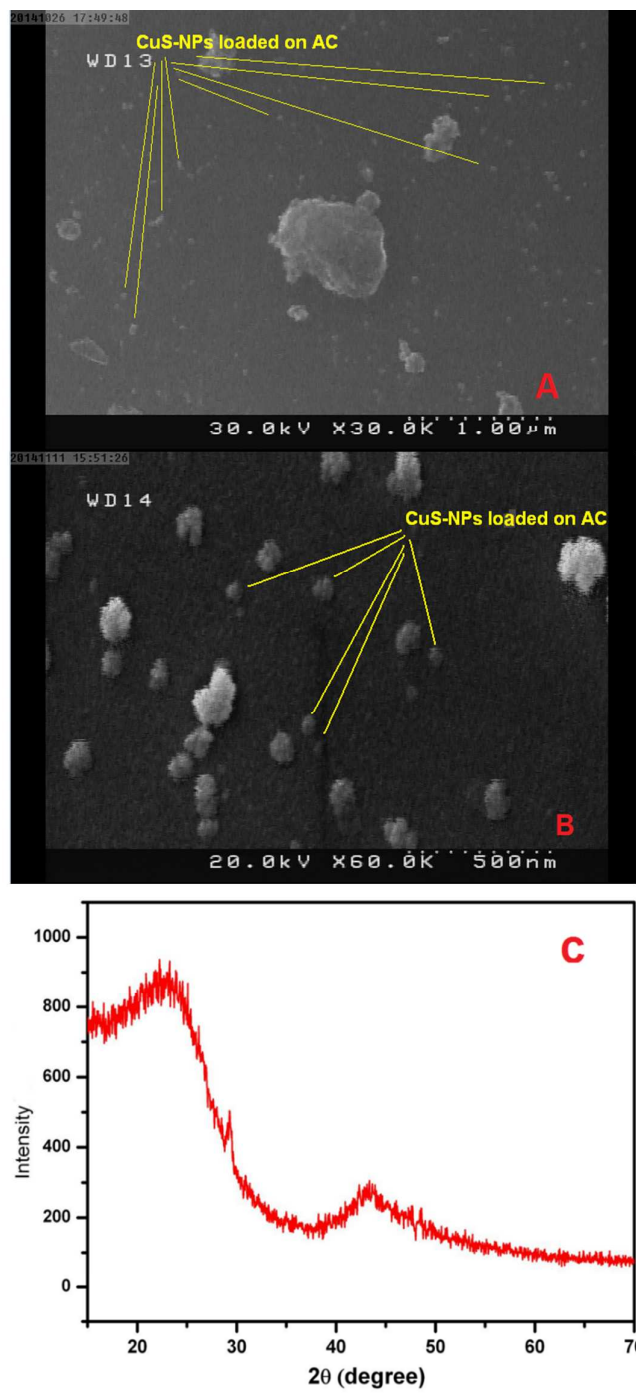


Fig 2.



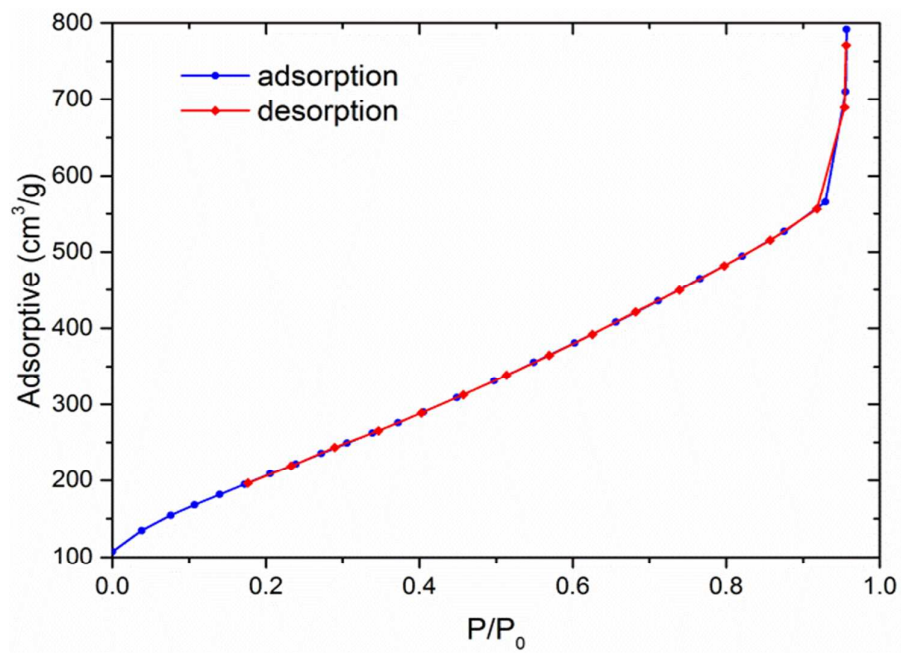


Fig. 3.

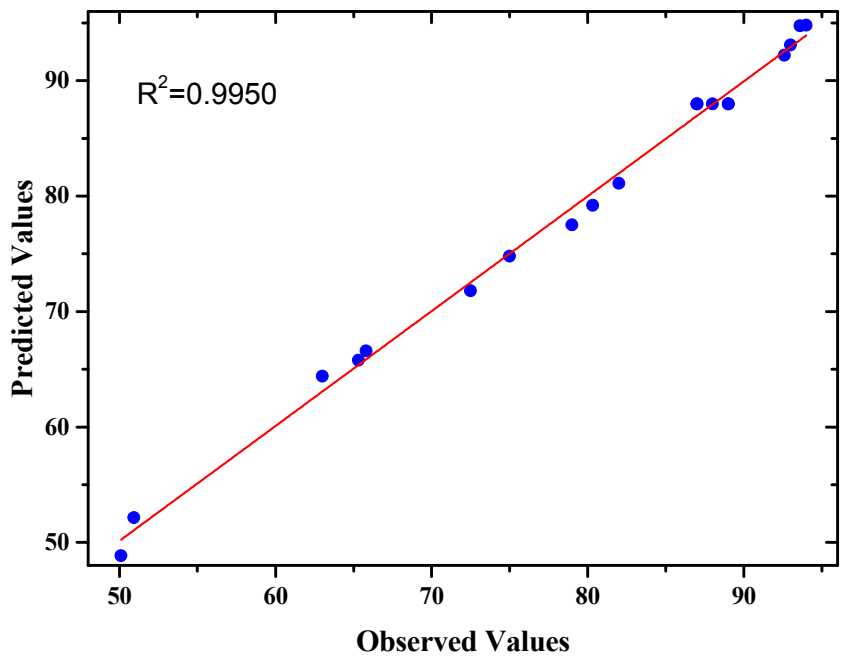


Fig.4.

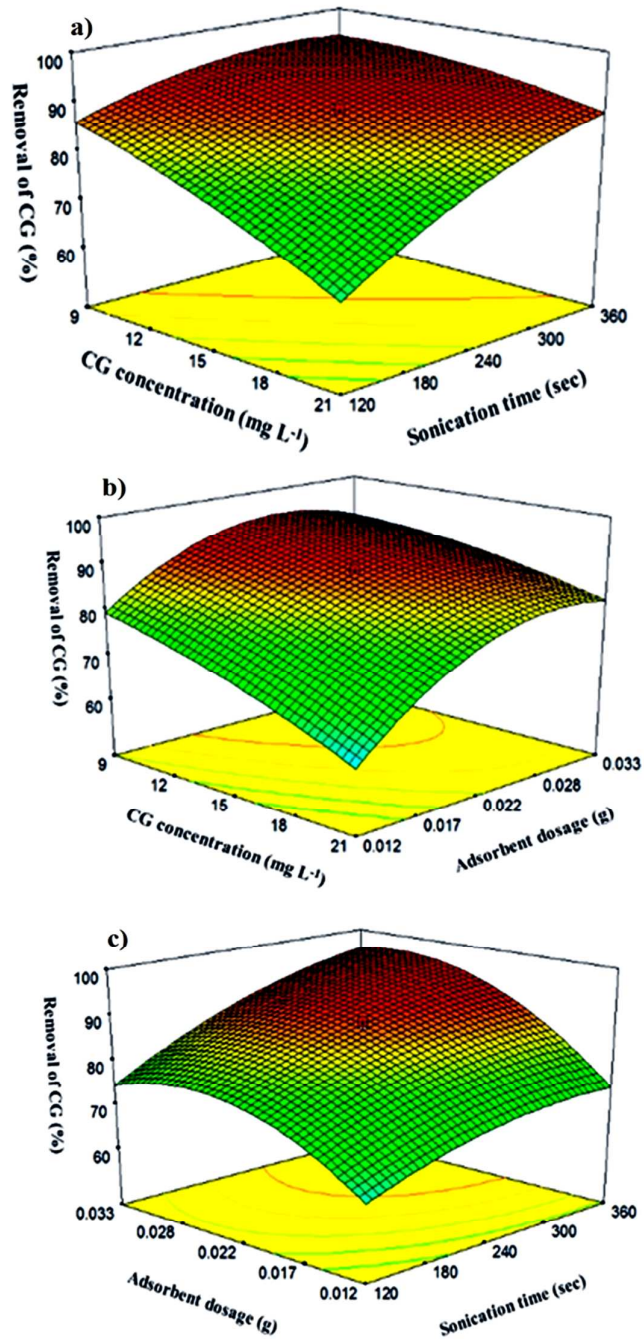


Fig.5.

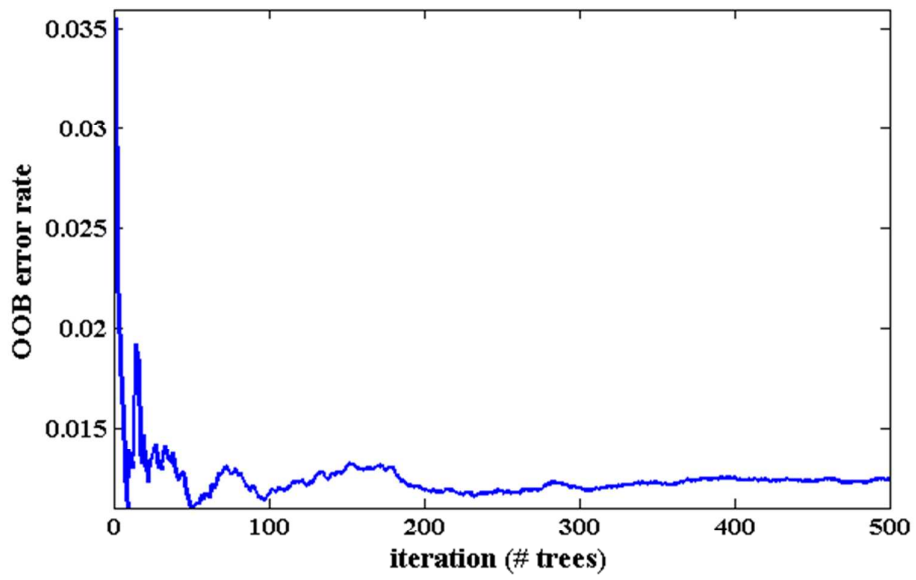


Fig. 6.